Journal of the Taiwan Institute of Chemical Engineers 000 (2018) 1–14

Contents lists available at ScienceDirect

Journal of the Taiwan Institute of Chemical Engineers

journal homepage: www.elsevier.com/locate/jtice

Using fuzzy inference system to predict Pb (II) removal from aqueous solutions by magnetic Fe_3O_4/H_2SO_4-activated *Myrtus Communis* leaves carbon nanocomposite

Hamedreza Javadian[a,*], Sanaz Asadollahpour[b], Montserrat Ruiz[c], Ana Maria Sastre[a], Maryam Ghasemi[d], Seyed Mostafa Hosseini Asl[e], Mojtaba Masomi[e]

[a] Department of Chemical Engineering, ETSEIB, Universitat Politècnica de Catalunya, Diagonal 647, 08028 Barcelona, Spain
[b] Institut für Organische Chemie, Universität Freiburg, Albertstraße 21, D-79104 Freiburg im Breisgau, Germany
[c] Department of Chemical Engineering, EPSEVG, Universitat Politècnica de Catalunya, Av. Víctor Balaguer, s/n, 08800 Vilanova i la Geltrú, Spain
[d] Young Researchers and Elite Club, Arak Branch, Islamic Azad University, Arak, Iran
[e] Department of Chemical Engineering, Ayatollah Amoli Branch, Islamic Azad University, Amol, Iran

ARTICLE INFO

Article history:
Received 20 January 2018
Revised 2 June 2018
Accepted 21 June 2018
Available online xxx

Keywords:
Magnetic nanoparticles
Myrtus Communis
Pb (II)
Adsorption
Desorption
Fuzzy inference system (FIS)

ABSTRACT

In this research study, a magnetic nanocomposite consisting of the Fe_3O_4 nanoparticles immobilized on *Myrtus Communis*-derived activated carbon (MM-AC) was synthesized and then, characterized by FE-SEM and FT-IR analytical methods. The results showed that the sizes of the Fe_3O_4 nanoparticles were about 54 nm, and the changes in the intensities of the major peaks were associated with the binding process. The adsorption efficiency of the MM-AC was evaluated for Pb (II) removal from aqueous solutions. The effective parameters such as pH, adsorbent dosage, contact time and initial metal ion concentration were optimized to reach maximum Pb (II) removal efficiency (%). The equilibrium amount of Pb (II) adsorbed onto the MM-AC suggested that the removal of Pb (II) followed Langmuir model. The kinetic studies on the removal of Pb (II) revealed that the adsorption process obeyed pseudo-second-order kinetic model. The maximum Pb (II) removal efficiency by the MM-AC was obtained at pH = 5. The adsorption capacity of Pb (II) onto the MM-AC changed from 88.65 to 480.90 mg/g by increasing the initial concentration of Pb (II) in the range of 100–400 mg/L. The comparison of maximum monolayer adsorption capacity of the MM-AC with other adsorbents reported in the literatures for removal of Pb (II) indicated that the MM-AC had better removal efficiency. In order to predict Pb (II) removal efficiency, a methodology based on fuzzy inference system (FIS) including multiple inputs and one output was developed. Four input variables namely pH, contact time (min), adsorbent dosage (g), and initial concentration of Pb (II) were fuzzified using an artificial intelligence-based approach. A Mamdani-type of fuzzy inference system was applied to implement a total of 18 rules in IF-THEN format along with a fuzzy subset consisting of a combination of Triangular and Trapezoidal membership functions in eight levels. The max-min method was employed as fuzzy inference operator, while defuzzification process was conducted using the center of gravity (COG, centroid) method. The achieved coefficient of determination value ($R^2 > 0.99$) confirmed the excellent accuracy of fuzzy logic model as a trustworthy prediction tool for Pb (II) removal efficiency. The overall results suggested that the developed material can be employed as an efficient adsorbent for Pb (II) removal from polluted aqueous solutions on a full-scale operation.

1. Introduction

In recent years, water pollution among other environmental pollutions has become one of the major problems in the world that must be controlled and reduced. By developing different industries such as microelectronics, metallurgical, battery manufacture, electroplating and fertilizer industries, variable quantities of heavy metals such as cadmium, chromium, copper, lead, mercury, nickel and arsenic are released into the environment. These heavy metals can be entered into surface water and groundwater by wastewaters and subsequently into the human body through different chains [1,2]. Among all the heavy metals, lead is one of the most toxic metals that can affect on the whole body and damage the central nervous system, kidney, liver and reproductive system. Due to its toxic effects and according to the World

* Corresponding author.
E-mail address: Hamedreza.javadian@upc.edu (H. Javadian).

https://doi.org/10.1016/j.jtice.2018.06.021
1876-1070/

Please cite this article as: H. Javadian et al., Using fuzzy inference system to predict Pb (II) removal from aqueous solutions by magnetic Fe_3O_4/H_2SO_4-activated *Myrtus Communis* leaves carbon nanocomposite, Journal of the Taiwan Institute of Chemical Engineers (2018), https://doi.org/10.1016/j.jtice.2018.06.021

Health Organization (WHO), the maximum permissible limit of lead in drinking water is 0.1 mg/L [3]. There are various methods such as reverse osmosis, chemical precipitation, adsorption, co-precipitation, membrane processes, ion exchange, photocatalysis, chemical oxidation/reduction, electrodialysis and ultra-filtration for wastewater treatment before discharging into the environment [4–6]. Considering the higher performance and ease of use, adsorption method is introduced as one of the widely used methods. In this method heavy metals are superficially adsorbed onto the surface of adsorbents, which are insoluble in water. The simplicity of adsorption method to obtain a high performance of wastewater treatment without any need to complicated processes as well as being selective for heavy metals are some of the advantages of this method [4]. Adsorption method using activated carbon and agricultural waste has the advantages of being cost-effective and efficient for removal of heavy metals from wastewaters. Activated carbons from biological materials are considered as efficient adsorbents due to their low cost and high adsorption capacity that is related to their high lingo-cellulosic contents [7]. In spite of these advantages, activated carbons are not easily separated from aqueous media; therefore, create secondary pollution. Using magnetic adsorbent is considered as an efficient method to easily separate them from aqueous phase by a simple magnetic field [8]. Magnetic adsorbents have been utilized in recent decades for the removal of metal ions, dyes and other molecules from water and wastewater because of having some features such as large surface area, large adsorption capacity, easy and rapid separation, reusable and favorable magnetic properties [9–13]. Immobilization technology along with the combination of adsorption and magnetic separation techniques can improve some features that mentioned above [14–17].

Myrtus Communis, commonly known as myrtle, is an evergreen shrub belonging to the Myrtaceae family that grows wild around the Mediterranean region. Its leaves are pleasantly scented, making it valuable for the perfume industry. It has white star-like delicate flowers and the fruit is a round, dark-blue berry containing the seeds. Many medicinal and nutraceutical properties have been attributed to myrtle, which has been used since ancient times in folk medicine. It is traditionally used as an antiseptic and wound-healing, disinfectant, hypoglycemic agent, with anti-hemorrhagic, antimicrobial and antioxidant properties [18]. It is also used in the food industries such as for flavoring meat and sauces, and in the cosmetic industries [19]. Ghaedi et al. used its activated carbon as an efficient adsorbent for congo red removal from aqueous solution [20].

Modeling is a valuable tool to assess effective parameters in various processes particularly the adsorption process. In fact, it not only helps in better understanding of the process procedure, but can also simulate the process with minimum experimental data. In an adsorption process, the operational conditions usually follow non-liner theoretical models. Therefore, the complex relationships between input and output parameters can be solved by means of non-liner methods known as computational intelligence methods [21]. The most reliable and powerful computational intelligence techniques include knowledge-based systems, neural networks, genetic algorithms, and fuzzy logic, which have attracted great attention as effective methods for environmental applications. In recent years, the prediction of adsorption processes has been conducted by various models such as artificial neural networks (ANN) [22], adaptive neuro-fuzzy inference system (ANFIS) [23], least squares support vector machines (LS-SVM) [24], random forest (RF) [25], response surface methodology (RSM) [26], genetic algorithm (GA) [27], and fuzzy inference system (FIS) [28].

Among the aforementioned models, fuzzy logic model introduced by Zadeh [29] is known as a suitable technique to develop environmental indices. It has a strong capability to convey human thoughts and experience in the form of indices, which can be calculated using uncertain, vague and subjective information. Also, the parameters with different amounts and meanings consisting both qualitative and quantitative variables can be precisely computed. Basically, fuzzy inference system (FIS) as a reliable method produces the results of an evaluation in the form of linguistic terms, which are comprehensible for managers, decision makers and non-experts [30]. There are few numbers of reported studies that used fuzzy logic (FL) approach to predict the uptake rate of heavy metals [31]. Rahmanian et al. [32] applied fuzzy logic model to predict Cr (VI) removal efficiency using micellar-enhanced ultrafiltration (MEUF). These studies clearly approve the applicability of fuzzy logic technique in different environmental matters particularly in the prediction of adsorption behavior.

In this research, *Myrtus Communis* leaves were chosen as cost-effectiveness source for the production of the M-AC. Then, the MM-AC nanocomposite was successfully produced by the immobilization of the Fe_3O_4 on the prepared activated carbon. According to our investigations, there have been no investigations of iron oxide magnetic nanoparticles (MNPs) immobilization on *Myrtus Communis* leaves activated carbon. FE-SEM and FT-IR techniques were applied to analyze the surface properties of the MM-AC. The adsorbent was tested for Pb (II) removal from aqueous solution. In addition, the kinetic and isotherm parameters were evaluated. A rule-based Mamdani type of fuzzy inference system was developed to predict Pb (II) removal efficiency. The proposed artificial intelligence-based model was validated using comparison between the fuzzy and experimental data under liner regression. Also, the influences of four input variables including pH, contact time (min), adsorbent dosage (g), and initial concentration of Pb (II) (mg/L) on Pb (II) removal efficiency were evaluated and the importance of each parameter was determined by sensitivity analysis.

2. Materials and methods

2.1. Reagents and instruments

Ferrous chloride tetrahydrate ($FeCl_2 \bullet 4H_2O$), ferric chloride hexahydrate ($FeCl_3 \bullet 6H_2O$), sodium hydroxide (NaOH), hydrochloric acid (HCl) and nitric acid (HNO_3) and sulfuric acid (H_2SO_4) were purchased from Sigma-Aldrich (St. Louis, MO, USA). The analytical grade of lead nitrate hexahydrate ($Pb(NO_3)_2 \bullet 6H_2O$, Merck Ltd, 99% purity) was employed to prepare a stock solution containing 1000 mg/L of Pb (II). The stock solution was diluted with deionized water to supply the desired concentrations of Pb (II). The pH of the solutions was adjusted using 0.1 M HNO_3 or 0.1 M NaOH. The FE-SEM (Model S4160, Hitachi, Japan) under a voltage of 20 kV and the FT-IR spectrometer (8400 s, Shimadzu, Japan) in the wavenumber range 4000–400 cm^{-1} were used for the characterization of the products. The Flame Atomic Absorption Spectrometer (GBC, SensAA Dual, Australia) with a lead hallow cathode lamp at the wavelength of 283.3 nm was used to monitor lead concentration in the solutions.

2.2. Preparation of MM-AC

2.2.1. Preparation of Myrtus Communis leaves activated carbon (M-AC)

At first, the collected *Myrtus Communis* leaves (Raw M) from Kermanshah were boiled in deionized water for 2 h to remove the water soluble phenolic and other organic compounds [20]. Then, they were washed several times with deionized water and dried at 110 °C in an air oven for 16 h to evaporate the moisture. Afterwards, they were crushed and sieved (40–60 mesh). Subsequently, 50 g of the sieved sample was taken into a 1 L beaker containing 50 g of concentrated sulfuric acid solution (weight ratio of 1:1). The mixture was dried at 110 °C in an air oven. The sulfuric

Please cite this article as: H. Javadian et al., Using fuzzy inference system to predict Pb (II) removal from aqueous solutions by magnetic Fe_3O_4/H_2SO_4-activated *Myrtus Communis* leaves carbon nanocomposite, Journal of the Taiwan Institute of Chemical Engineers (2018), https://doi.org/10.1016/j.jtice.2018.06.021

acid-treated *Myrtus Communis* was placed in the ceramic crucibles and kept in the furnace. Then, the temperature of the furnace was increased under N_2 gas from room temperature to 400 °C with a retention time of 3 h. Finally, M-AC was washed with deionized water several times and the neutralized sample was dried in an air oven at 100 °C.

2.2.2. Preparation of MM-AC

The MM-AC was prepared by co-precipitation method by the following procedure: 100 mL solution consisting of $FeCl_3 \bullet 6H_2O$ and $FeCl_2 \bullet 4H_2O$ with the molar ratio of 2:1 along with 10 g of M-AC was stirred magnetically. Subsequently, 50 mL of sodium hydroxide (0.5 M) was added dropwise to the mixture under N_2 gas until the pH value reached to 11. This mixture was agitated for 30 min, and the composite was separated via centrifugation. Then, it was washed with deionized water and dried at 50 °C for 24 h in an air oven. Finally, it was heated at 200 °C for 4 h under N_2 gas.

2.3. Batch adsorption experiments

In order to investigate Pb (II) removal from aqueous solution, the experiments were performed in the 250 mL beakers containing a certain amount of the MM-AC with a given Pb (II) concentration and pH value by stirring at 350 rpm at room temperature (298 K). For the batch adsorption tests, the variables were investigated in the pH range of 1–7, the contact time of 1, 3, 6, 9, 12, 15, 20, 30, 50, 80 and 120 min, the MM-AC dosage of 0.001, 0.005, 0.01, 0.015 and 0.02 g, and the Pb (II) initial concentration of 30, 50, 70, 100, 150, 200, 300, and 400 mg/L.

After ending the contact time, the adsorbent was separated by a magnetic field and then, the residual Pb (II) in the solution was analyzed by the atomic absorption spectrometer.

The adsorption capacity and Pb (II) removal efficiency by the MM-AC were calculated by the following equations:

$$q_e = \frac{C_0 - C_e}{m} \times V \tag{1}$$

$$\%Removal = \frac{C_0 - C_e}{C_0} \times 100 \tag{2}$$

where, C_0 and C_e (mg/L) represent the concentrations of Pb (II) at initial and a given time t, V is the volume of the solution and m the dosage of the MM-AC.

2.4. Desorption and regeneration study

Desorption and regeneration study is a key factor that is needed to be performed to make the adsorption process more economical. For desorption experiments, 0.1 M HCl was used. To show the reusability of the adsorbent, adsorption–desorption cycle was repeated five times under the same conditions.

2.5. Kinetics studies

Normally, adsorption kinetics describe the solute uptake rate at the solid-solution interface and evidently provide information about the reaction pathways and mechanisms. The kinetics of Pb (II) adsorption onto MM-AC were analyzed using pseudo-first-order [33,34], pseudo-second-order [35] and intra-particle diffusion [36] models. The conformity between the experimental data and the values predicted by the models was expressed by coefficient of determination (R^2) [33].

2.6. Adsorption isotherm

The analysis of isotherm data is important to develop an equation that accurately represents the results to design adsorption process. In order to investigate the adsorption isotherm, four equilibrium models were applied. Langmuir [37] and Freundlich [33] isotherms were used as the most two-parameter models. Temkin [38] and Dubinin-Radushkevich [4] isotherms were used for determination of the energy of Pb (II) adsorption.

2.7. Fuzzy logic theory

Fuzzy logic is known as an alternative and applicable method for developing both linear and nonlinear relationships between input-output variables. In industrial scale, fuzzy logic model provides accurate predictions that lead to the reduction of operational costs, better performance of units and ultimately high level of quality in products. Fuzzy logic model follows fuzzy set theory defined based on uncertain reasoning instead of accurate deduction of classic predicate. In fact, the strength of fuzzy logic is in the emulation of human mind and using approximate modes of reasoning. Making decision in fuzzy logic, as a soft computing method, is along with tolerance and perception because the mapping rules are determined in the form of terms (words) instead of numbers. One of the benefits associated with fuzzy logic is the modeling of various systems with multiple input-output variables. Zadeh [29] introduced the fuzzy logic term for the first time and represented mathematic relationships in fuzzy set theory, which clearly confirmed the existence of a third region apart from True and False. The approximate reasoning of fuzzy technique is obtained from the expert knowledge transforming to fuzzy rules format. These fuzzy rules are converted to mathematic equivalents by fuzzy systems. This transformation not only helps to better understanding of the procedure, but also leads to precise and real outcomes of a model. Therefore, the decision support systems of a fuzzy logic model have powerful reasoning capabilities for dealing with the conditions that are inherently imprecise [39].

The simplicity and flexibility of fuzzy logic model makes it to one of the most suitable tools in the field of prediction. As shown in Fig. 1, each fuzzy inference system (FIS) contains four fundamental units including fuzzification unit, knowledge base unit that is composed of data base and rule base, inference engine unit, and defuzzification unit. The two major approaches of fuzzy inference system are Mamdani and Sugeno methods that can be applied for various purposes like control and prediction [40,41]. In both approaches, the main procedure is the same as fuzzification, inference and defuzzificiation, but there are some differences between Mamdani and Sugeno approaches in defuzzification part. In the Sugeno approach, the outcome of each IF-THEN rule is a scalar that is either constant or a liner function for output variable, and defuzzification procedure is accomplished by calculating the weighted average of the rule outcome. On the other hand, the result of every IF-THEN rule in the Mamdani method is the production of a fuzzy set for the output variable which can easily merge the linguistic information into model. Furthermore, the existence of defuzzification step is essential for achieving crisp values of the output variable. Mamdani models are known as more appropriate approaches for modeling qualitative information; thus, it was applied in this study. The most significant concepts of fuzzy inference process are the membership functions, fuzzy set operations and inference rules that are explained extensively in the following sections.

2.7.1. Membership functions

A fuzzy set is a format of a crisp set where a characteristic function $\mu_A(x)$ is defined based on the membership or

Please cite this article as: H. Javadian et al., Using fuzzy inference system to predict Pb (II) removal from aqueous solutions by magnetic Fe_3O_4/H_2SO_4-activated *Myrtus Communis* leaves carbon nanocomposite, Journal of the Taiwan Institute of Chemical Engineers (2018), https://doi.org/10.1016/j.jtice.2018.06.021

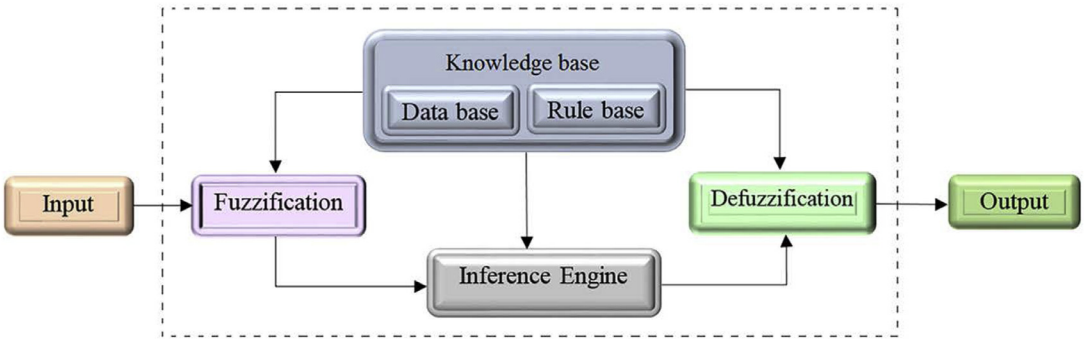

Fig. 1. Fuzzy inference system approach.

non-membership of element x in set A.

$$\mu_A(x) = 1 \; if \; x \in A, \qquad \mu_A(x) = 0 \; if \; x \notin A \tag{3}$$

This concept was extended using the definition of partial membership in fuzzy set theory. It states that a fuzzy set A as a set of ordered pairs is a subset of the universe of discourse X that is described by a membership function $\mu_A(x)$ with values in the range between 0 and 1.

$$A = \{(x, \mu_A(x)) | x \in X\} \; 0 \le \mu_A(x) = 1 \tag{4}$$

where x belongs to X and $\mu_A(x)$ is the membership function of x in fuzzy set A. Basically, a membership function is a curve that characterizes how every point in the input space (universe of discourse) is plotted versus output-axis (membership value μ) between 0 and 1. In the other words, the amounts of each variable is expressed by the membership functions of a fuzzy set in the form of general linguistic labels such as “Very Low”, “Low”, “Medium”, “High”, “Very High”, etc. One of the benefits of fuzzy inference system is that the membership of a determined element can be present simultaneously in several fuzzy sets. There are different types of membership functions such as triangular, trapezoidal, generalized bell shaped, Gaussian curves, polynomial curves, and sigmoid functions [42]. The most important factors for determining the shape of a membership function are expert knowledge and expected accuracy of designer from fuzzy results. For this purpose, some usable methods like fuzzy clustering, neural networks and genetic algorithms are also introduced.

2.7.2. Fuzzy set operations

Fuzzy set operators are responsible for determining the relationships between fuzzy subsets. The fuzzy logic operators are considered as crisp set operators whose allocated fuzzy values; 1 (True) or 0 (False), follow their equations. In order to develop various rule-based fuzzy logic systems, there are multiple fuzzy set operators used for managing the essence of fuzzy logic. The standard fuzzy set operations are union (OR), intersection (AND), and negation (NOT). If there are two fuzzy sets A and B as the subsets of universe X, for a given element x belonging to X, the fuzzy set operators are defined by the following equations:

$$\begin{aligned}(\text{Intersection, AND}) : \mu_{A\cap B}(x) &= \mu_A(x) \cap \mu_B(x) \\ &= \min(\mu_A(x), \mu_B(x))\end{aligned} \tag{5}$$

$$(\text{Union, OR}) : \mu_{A\cup B}(x) = \mu_A(x) \cup \mu_B(x) = \max(\mu_A(x), \mu_B(x)) \tag{6}$$

$$(\text{Negation, NOT}) : \mu_{\bar{A}}(x) = 1 - \mu_A(x) \tag{7}$$

The aforementioned operators are known as the basic operators in a fuzzy inference system. The aggregation process is carried out using these operators and the desired results are obtained in most of the times [39].

2.7.3. Inference rules

Inference rules, as the third concept, play a significant role in fuzzy inference systems. They define the relationship between fuzzy subsets of inputs and outputs using IF-THEN rules which leads to the production of a new output subset. The general format of an IF-THEN rule is as follows:

$$\text{Rule}_{(i)} : \text{If X is } A_i \text{ and Y is } B_i, \ldots \text{then Z is } C_i, \ldots, \; i = 1 \ldots n \tag{8}$$

where A_i, B_i, and C_i are defined as the linguistic variables of fuzzy sets in the universes of discourse *X*, *Y* and *Z*, respectively. As exhibited above, every rule has two parts; if- part (antecedent or premise) and then- part (consequent or conclusion), each of which can be composed of several sections. Therefore, there are two steps with distinct interpretations for each IF-THEN rule. In the first step, an antecedent is evaluated and the input is fuzzified using specified fuzzy operators and then (the second step; implication), the outcomes of antecedent is applied to the consequent and as a result, the membership function is essentially examined.

3. Results and discussion

3.1. Characterization of the synthesized materials

Fig. 2a–c show the FE-SEM images of the Raw M, M-AC and MM-AC in different magnifications. It can be seen from Fig. 2a that the leaf has a smooth surface without any porosity. Fig. 2b shows that acid sulfuric activation process created porous surface with the holes in different sizes that can be used for Pb (II) adsorption. In Fig. 2c, the Fe_3O_4 particles completely covered the M-AC surface that is roughly spherical in shape and uniform in distribution. As shown in Fig. 2c, the Fe_3O_4 nanoparticles are about 54 nm in diameter. Fig. 2d shows that the morphology of the MM-AC is changed by Pb (II) adsorption.

The FT-IR spectra of the Raw M and M-AC are given in Fig. 3. Fig. 3a indicates that the Raw M has several absorption peaks. The peak around 3440 cm^{-1} is attributed to C–OH groups. The two peaks at 2854 (υ_s C–H) and 2931 cm^{-1} (υ_a C–H) are related to stretching vibration of C–H. The peak at 2360 cm^{-1} is assigned to N–H bond. The peak around 1643 cm^{-1} is assigned to an aromatic carbon or carboxyl groups. The intense peak at 1049 cm^{-1} is related to alcohol groups (R–OH). After activation process, the two new peaks at 678 and 617 cm^{-1} are assigned to out of plane N–H and C–S groups, respectively (Fig. 3b) [43]. The FT-IR spectrum of MM-AC is shown in Fig. 3c. The intense peak at 1164 cm^{-1} is attributed to C–OH stretching. The presence of peak at 577 cm^{-1} confirms that the Fe_3O_4 particles were coated on M-AC [44]. In Fig. 3d, the changes in the intensity of the peaks show that a

Please cite this article as: H. Javadian et al., Using fuzzy inference system to predict Pb (II) removal from aqueous solutions by magnetic Fe_3O_4/H_2SO_4-activated *Myrtus Communis* leaves carbon nanocomposite, Journal of the Taiwan Institute of Chemical Engineers (2018), https://doi.org/10.1016/j.jtice.2018.06.021

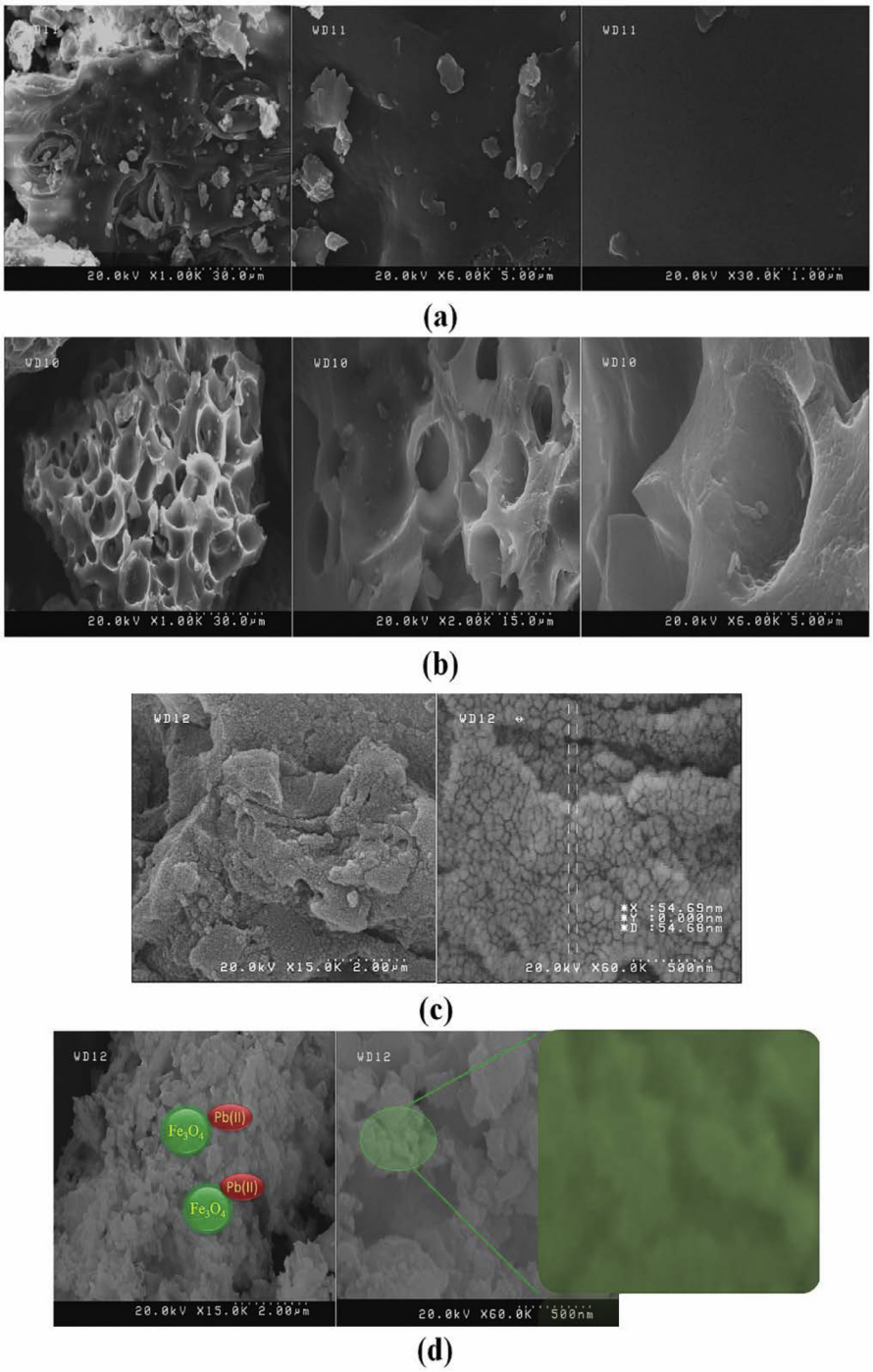

Fig. 2. FE-SEM images of the (a) Raw M (b) M-AC (c) MM-AC and (d) Pb (II)–MM-AC.

binding process was taken place on the surface of the MM-AC after Pb (II) adsorption. Table 1 shows the wavenumbers for the different functional groups presenting in the Raw M, M-AC and MM-AC and Pb (II)-MM-AC.

3.2. Effects of pH and adsorbent dosage

The effect of pH on the removal efficiency and uptake (q_e) of Pb (II) was investigated in the range of 1–7. As shown in Fig. 4a, the removal efficiency and uptake of Pb (II) significantly increases by changing pH value in the range of 1–5. By increasing pH value from 1 to 5, Pb (II) removal efficiency increases from 5.33 to 89.11%. Similarly, the Pb (II) adsorption capacity increases from 15 to 250.50 mg/g by increasing pH value from 1 to 5. The low uptake of Pb (II) is observed at lower pH value that can be attributed to the large quantities of protons competing with Pb (II) ions for the adsorption sites. This can be explained that by increasing pH value, more positively charged Pb (II) ions are adsorbed by free binding sites due to a larger portion of dissociation of protons from functional groups, resulting in the promotion of adsorption capacity [16]. At pH = 5, the maximum Pb (II) removal efficiency of 89.11% by the MM-AC is obtained that can be attributed to the available lead species at pH = 5; therefore, it can be adsorbed by the available sites on the MM-AC surface. Thus, pH = 5 was considered as an optimum value for further studies.

Please cite this article as: H. Javadian et al., Using fuzzy inference system to predict Pb (II) removal from aqueous solutions by magnetic Fe_3O_4/H_2SO_4-activated *Myrtus Communis* leaves carbon nanocomposite, Journal of the Taiwan Institute of Chemical Engineers (2018), https://doi.org/10.1016/j.jtice.2018.06.021

Table 1
Wavenumbers (cm^{-1}) for the peaks from FT-IR spectroscopy.

Functional groups	Raw M	M-AC	MM-AC	Pb (II)–MM-AC
C–OH group	3471	3440	3417	3425
Stretching vibration of C–H	2923, 2877	2931, 2854	2931, 2854	2923, 2854
N–H bond	2360	2360	–	–
Aliphatic acid C = O stretching	–	1743	1720	1712
Aromatic carbon or carboxyl groups	1604	1643	1627	1620
O–H bending	–	–	1388	1388
C–H bending	–	1164	–	–
C–OH stretching	1049	–	–	–
Fe–O groups	–	–	577	577

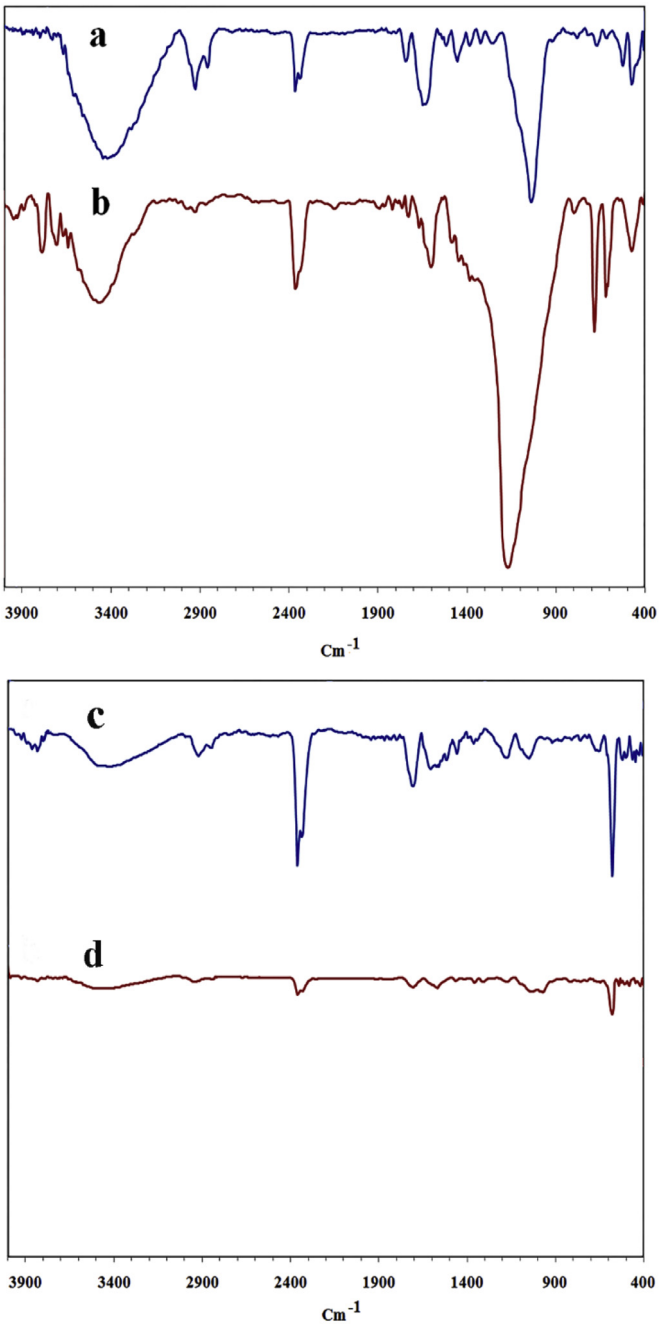

Fig. 3. FT-IR spectra of the (a) Raw M (b) M-AC, (c) MM-AC, and (d) Pb (II)–MM-AC.

Adsorbent dosage is a key parameter in the determination of removal efficiency and adsorption capacity. As the adsorbent dosage is increased, the available adsorbent sites are also increased; consequently, a better adsorption takes place [45]. In this study, the adsorbent dosage was increased from 1 to 20 mg, while pH, contact time and Pb (II) concentration were kept at a constant value. The effect of the MM-AC dosage on the removal efficiency and uptake of Pb (II) from aqueous solution is shown in Fig. 4b. Fig. 4b shows an increase in the removal efficiency from 54.3 to 89.11% by increasing the adsorbent dosage from 1 to 20 mg. This result can be attributed to the fact that by increasing the adsorbent dosage, the density of the available reactive groups on the surface of the adsorbent for metal binding increases. According to Fig. 4b, the adsorption capacity decreases by increasing the adsorbent dosage. As the adsorbent dosage increases from 1 to 20 mg, decreasing in Pb (II) adsorption capacity from 1629 mg/g to 133.57 mg/g is observed. The decrease in adsorption capacity may be due to the interference existed between the binding sites and adsorbent, or the insufficiency of Pb (II) ions in the solution with respect to available binding sites [16].

3.3. Effect of contact time

The effect of contact time on the removal efficiency and uptake of Pb (II) from aqueous solution onto the MM-AC is shown in Fig. 4c. It is observed that by increasing contact time from 1 to 120 min, the adsorption capacity of Pb (II) increases from 337.75 to 412.75 mg/g. More than 60% of Pb (II) is adsorbed within 1 min; accordingly, it can be mentioned that the removal efficiency and uptake of Pb (II) is rapid at the beginning of the adsorption process due to a large number of active sites being available on the adsorbent surface for Pb (II) adsorption [46].

3.4. Kinetic studies

The obtained data from adsorption of Pb (II) onto the MM-AC were fitted to pseudo-first-order, pseudo-second-order, and intra-particle diffusion and the results are summarized in Table 2. According to Table 2, it is evident that coefficient of determination (R^2) value obtained by pseudo-first-order model (0.711) is small, and the experimental q_e value is not in agreement with the calculated value. As can be seen from Table 2, for Pb (II) adsorption onto the MM-AC, the obtained coefficient of determination (R^2) value by pseudo-second-order model is higher than that of pseudo-first-order model. Furthermore, the q_e values indicate a good agreement between the experimental and calculated q_e values. Thus, pseudo-second-order model is appropriate for predicting the adsorption process. The coefficient of determination (R^2) of intra-particle diffusion is 0.89, suggesting that two or more steps are involved in Pb (II) adsorption onto the MM-AC. The low values of R^2 obtained from pseudo-first-order and intra-particle

Please cite this article as: H. Javadian et al., Using fuzzy inference system to predict Pb (II) removal from aqueous solutions by magnetic Fe_3O_4/H_2SO_4-activated *Myrtus Communis* leaves carbon nanocomposite, Journal of the Taiwan Institute of Chemical Engineers (2018), https://doi.org/10.1016/j.jtice.2018.06.021

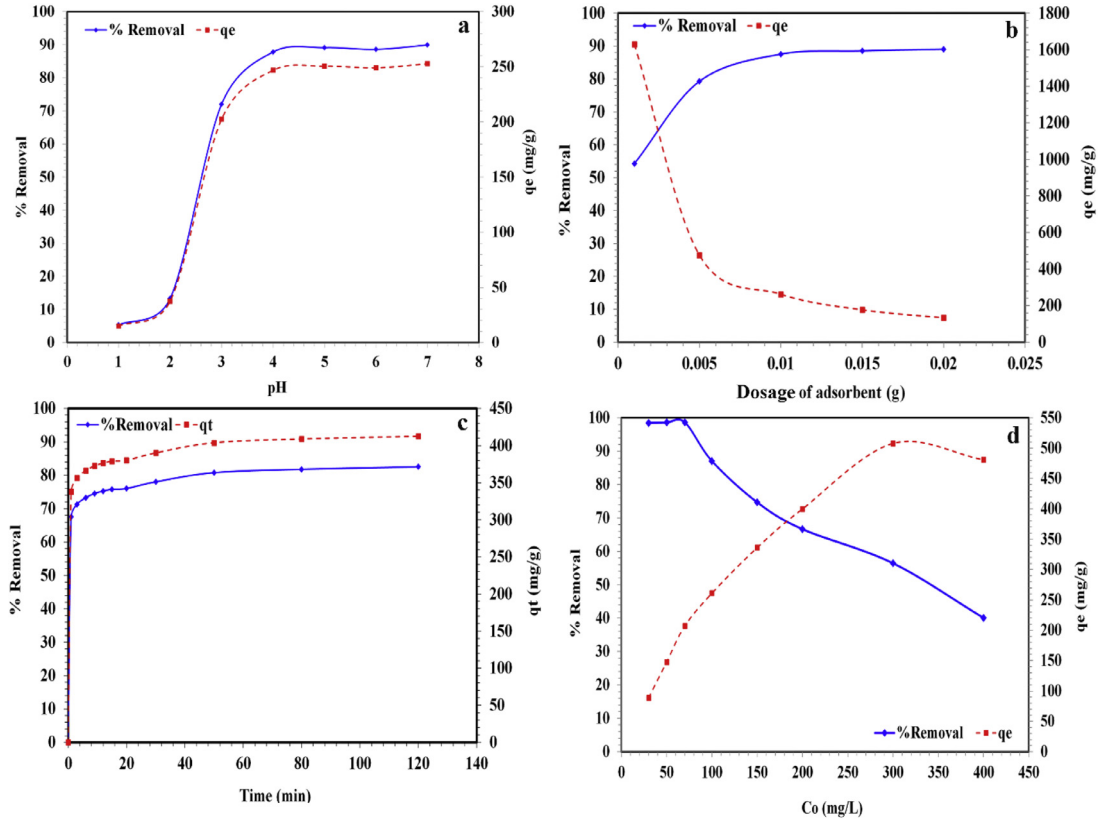

Fig. 4. (a) Effect of (a) pH, (b) adsorbent dosage, (c) contact time and (d) initial concentration on Pb (II) adsorption by the MM-AC.

Table 2
Adsorption kinetics of Pb (II) onto the MM-AC.

Model	Parameter	Initial concentration (mg/L) 100
Pseudo-first-order $\log(q_e - q_t) = \log q_e - (\frac{k_1}{2.303})t$	$q_{e(exp)}$ (mg/g)	419
	q_e (mg/g)	77.037
	k_1 (min^{-1})	0.024
	R^2	0.711
Pseudo-second-order $\frac{t}{q_t} = \frac{t}{q_e} + \frac{1}{k_2 q_e^2}$	$q_{e(exp)}$ (mg/g)	419
	q_e (mg/g)	416.66
	k_2 (g/mg.min)	0.002
	$h = k_2 q_e^2$ (initial adsorption rate)	347.21
	R^2	0.999
Intra-particle diffusion $q_t = k_i t^{0.5} + c$	K_i (mg/g.min)	6.938
	C (mg/g)	347.4
	R^2	0.893

diffusion models indicate the unsuitability of these models for predicting the adsorption of Pb (II) onto the MM-AC.

3.5. Effect of initial concentration

The effect of Pb (II) initial concentration on its removal efficiency is shown in Fig. 4d. The removal efficiency of Pb (II) decreases by increasing its initial concentration. When the concentration of Pb (II) is lower than 100 mg/L, the removal efficiency is about 98% due to a large surface area of MM-AC being available for Pb (II) adsorption. The removal efficiency of Pb (II) decreases from 87 to 40% by increasing initial concentration from 100 to 400 mg/L. The removal efficiency is low at higher concentration of Pb (II) due to the lower available adsorption sites in comparison with the number of Pb (II) ions. In this study, the performance of the MM-AC was evaluated by its maximum adsorption capacity. The adsorption capacity of the MM-AC changes from 88.65 to 480.90 mg/g by increasing Pb (II) initial concentration from 100 to 400 mg/L. The higher initial concentration of Pb (II) provides a driving force to overcome the mass transfer resistance between the aqueous and solid phases [33].

3.6. Adsorption isotherms

The parameters obtained from fitting the data to Langmuir, Freundlich, Temkin and Dubinin-Radushkevich isotherm models are shown in Table 3. According to Table 3, the best fit is obtained by Langmuir Type 1 ($R^2 = 0.991$) in comparison with its other models. The maximum monolayer capacity of Pb (II) adsorption onto the MM-AC obtained by Langmuir Type 1, Type 2, Type 3 and Type 4 are 500.0, 416.6, 408.3 and 258.5 mg/g, respectively. The R_L value indicates the adsorption nature to be either unfavorable ($R_L > 1$), linear ($R_L = 1$), favorable ($0 < R_L < 1$) and irreversible ($R_L = 0$). The R_L values in Table 3 are in the range of 0–1, indicating a favorable isotherm shape for Pb (II) adsorption onto the MM-AC. A value of $n > 1$ indicates that adsorption is favorable [38]. The value of n

Please cite this article as: H. Javadian et al., Using fuzzy inference system to predict Pb (II) removal from aqueous solutions by magnetic Fe_3O_4/H_2SO_4-activated *Myrtus Communis* leaves carbon nanocomposite, Journal of the Taiwan Institute of Chemical Engineers (2018), https://doi.org/10.1016/j.jtice.2018.06.021

Table 3
Adsorption isotherms of Pb (II) ions onto the MM-AC.

Model		Parameter	Value
Langmuir $q_e = \frac{bK_LC_e}{1+bC_e}$	Type 1 $\frac{C_e}{q_e} = \frac{1}{bK_L} + \frac{C_e}{b}$	K_L (L/mg)	0.141
		b (mg/g)	500
		R^2	0.991
		R_L	0.074
	Type 2 $\frac{1}{q_e} = (\frac{1}{bK_L})\frac{1}{C_e} + \frac{1}{b}$	K_L (L/mg)	0.685
		b (mg/g)	416.66
		R^2	0.927
		R_L	0.016
	Type 3 $q_e = b - (\frac{1}{K_L})\frac{q_e}{C_e}$	K_L (L/mg)	0.797
		b (mg/g)	408.34
		R^2	0.723
		$R_L = \frac{1}{1+K_LC_o}$	0.014
	Type 4 $\frac{q_e}{C_e} = K_Lb - K_Lq_e$	K_L (L/mg)	0.576
		b (mg/g)	258.5
		R^2	0.723
		R_L	0.019
Freundlich $\log q_e = \log K_f + \frac{1}{n}\log C_e$		K_f	150.072
		$1/n$	0.230
		n	4.347
		R^2	0.902
Temkin $q_e = B\ln A + B\ln C_e$		A	14.882
		$B = \frac{RT}{b_T}$	59.052
		$B \ln A$	159.45
		R^2	0.934
Dubinin–Radushkevich $\ln q_e = \ln q_m - K_D\varepsilon^2$ $\varepsilon = RT\ln(1+\frac{1}{C_e})$		K_D	0.181
		q_m	382.412
		$E = \frac{1}{\sqrt{2K_D}}$	1.662
		R^2	0.883

is 4.347, showing that there is a strong interaction between the MM-AC and Pb (II). The value of $E < 8$ kJ/mol describes physical adsorption and the value of E between 8 and 16 kJ/mol is related to chemical ion-exchange [47]. The low E value clearly indicates that Pb (II) adsorption onto the MM-AC is mainly through physical adsorption. Among all isotherm models, Langmuir Type 1 shows the highest coefficient of determination (R^2) value, suggesting the monolayer coverage of Pb (II) and its adsorption at specific available homogeneous sites on the surface of the MM-AC. The R^2 values of 0.90, 0.93 and 0.88 obtained from fitting the data to Freundlich, Temkin and Dubinin–Radushkevich models, respectively, indicate that these models are not suitable for predicting Pb (II) adsorption onto the MM-AC.

Generally, oxygen-containing functional groups can strengthen the interactions between adsorbents and adsorbate by forming surface complexes, cation-π bonding, electrostatic attraction and/or ion exchange, resulting in faster adsorption rate and higher adsorption ability [48–51]. The enhanced adsorption of Pb (II) by the MM-AC allows us to propose the following mechanism shown in Scheme 1 to explain the latitude of this material for metal chelation via the partial negative charges of oxygen atoms. Although this mechanism allows us to visualize the possible chemical interactions, which makes the prepared magnetic composite as an efficient adsorbent for Pb (II) removal, there can be other kinds of interaction mechanisms.

3.7. Desorption and regeneration study

The desorption and regeneration of the MM-AC were performed five times to investigate its reusability, and the results are shown in Fig. 5. It is evident that after five consecutive cycles, Pb (II) removal efficiency decreases from 87.30 to 81.55% and its desorption efficiency decreases from 86.48 to 75.30%. The results show that the MM-AC can be efficiently utilized several times for Pb (II) removal.

3.8. Comparison of the MM-AC with the adsorbents reported in the literatures

The maximum monolayer adsorption capacity of the MM-AC was compared with some adsorbents used for Pb (II) removal. The reported results in Table 4 show that the maximum monolayer adsorption capacity of the MM-AC is greater than that of other adsorbents; thus, it can be mentioned that MM-AC has a great potential for Pb (II) removal from aqueous solutions.

3.9. Development of fuzzy model

The rule-based fuzzy logic model was developed to predict Pb (II) removal efficiency from aqueous solutions by the MM-AC. The model was designed based on evaluated parameters in actual conditions of the experiments. Four input variables including pH, adsorbent dosage (g), contact time (min) and Pb (II) initial concentration (mg/L) were defined for the model in the ranges of [0,8], [0,20], [0,120] and [0,400], respectively. On the other hand, Pb (II) removal efficiency was the only output variable determined in the range of [0, 100]. Eight fuzzy sets (VVL, VL, L, M, MH, H, VH, VVH) namely “very very low”, “very low”, “low”, “medium”, “medium high”, “high”, “very high” and “very very high” were selected for input variables (pH, D, t, C). Also, multiple membership functions (VL, L, LM, M, M(1), MH, MH(1), H, VH, VVH) namely “very low”, “low”, “low medium”, “medium”, “medium one”, “medium high”, “medium high one”, “high”, “very high” and “very very high” were considered for removal efficiency as output variable. Trapezoidal and triangular membership functions were applied to define these fuzzy sets (Fig. 6a). Use of these two types of membership functions provides less computation time rather than other types. In addition, they can work very well particularly in a system with several fuzzy sets with 15% to 25% overlap of adjacent sets [55]. The trapezoidal curves rely on four parameters (a, b, c, d), while the triangular curves work with three parameters (a, b, c) as demonstrated in the following equations:

$$f(x,\ a,\ b, c, d) = \begin{cases} 0 & x < a \\ \frac{x-a}{b-a} & a \le x < b \\ 1 & b \le x < c \\ \frac{d-x}{d-c} & c \le x < d \\ 0 & d \le x \end{cases} \quad (9)$$

$$f(x,\ a,\ b, c) = \begin{cases} 0\ x \le a \\ or \\ x \ge c \\ \frac{x-a}{b-a}\ a \le x \le b \\ \frac{c-x}{c-b}\ b \le x \le c \end{cases} \quad (10)$$

The compact forms of above functions are presented below. In trapezoidal membership functions, b and c are located at the “top” of trapezoid, while a and d are set at the “bottom”. Also, a and c in triangular membership functions are at the “feet” of triangle and b is at the “peak”.

$$\text{Trapezoidal}: f(x, a, b, c, d) = \max\left(\min\left(\frac{x-a}{b-a}, 1, \frac{d-x}{d-c}\right), 0\right) \quad (11)$$

$$\text{Triangular}: f(x, a, b, c) = \max\left(\min\left(\frac{x-a}{b-a}, \frac{c-x}{c-b}\right), 0\right) \quad (12)$$

3.9.1. Fuzzy model mechanism

The Mamdani type of fuzzy inference system (FIS) employed in this study follows a four-step mechanism consisting of fuzzification of the input variables, rule evaluation, aggregation of the rule

Please cite this article as: H. Javadian et al., Using fuzzy inference system to predict Pb (II) removal from aqueous solutions by magnetic Fe_3O_4/H_2SO_4-activated *Myrtus Communis* leaves carbon nanocomposite, Journal of the Taiwan Institute of Chemical Engineers (2018), https://doi.org/10.1016/j.jtice.2018.06.021

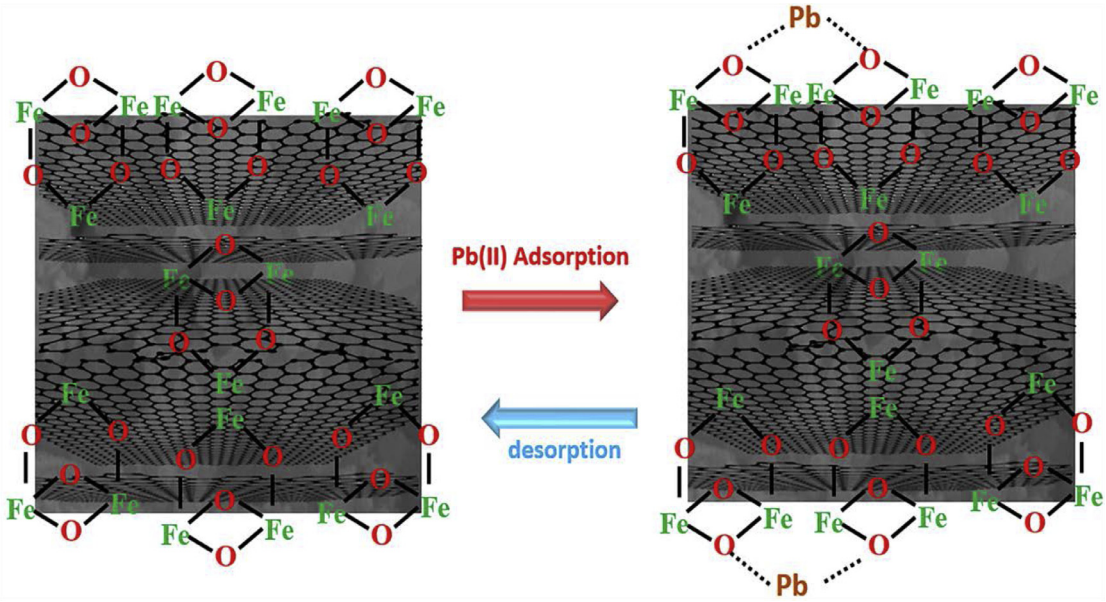

Scheme 1. Proposed mechanism of Pb (II) adsorption onto the MM-AC.

Table 4
Comparison of the maximum monolayer adsorption (b) of Pb (II) onto various adsorbents.

Adsorbent	*b* (mg/g)	Ref.
Magnetite nanoparticles	3.44	[9]
Polymer-modified magnetic nanoparticles	166.1	[12]
Iron oxide nanoparticles immobilized *Phanerochaete chrysosporium*	176.33	[13]
Nano zerovalent iron nanoparticles graphene composite	585.5	[15]
Iron oxide nanoparticles immobilization of *Phanerochaete chrysosporium*	185.25	[16]
Chitosan/magnetite nanocomposite beads	63.33	[17]
Magnetic alginate beads based on maghemite nanoparticles	50	[52]
Amino-functionalized magnetic nano adsorbent	40.10	[53]
Fe_3O_4@SiO_2–NH_2nanoparticles	361.01	[54]
MM-AC	500	This study

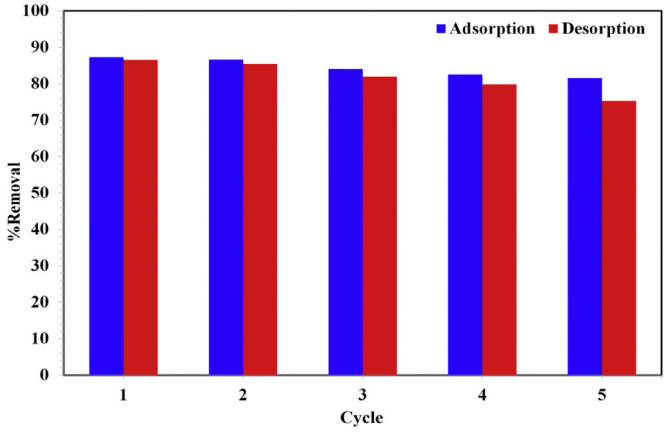

Fig. 5. Adsorption–desorption cycles.

outputs, and defuzzification. After establishing the rules based on expert knowledge, the vectors of input-output are mapped by the fuzzy inference system (Fig. 6b). In the first step, the fuzzifuier takes crisp inputs (numbers) and determines their degree using the selected membership functions for finding appropriate fuzzy sets corresponding to input values. The next step is rule evaluation in which the fuzzified inputs are applied as the antecedents of the fuzzy rules. If a fuzzy rule has several antecedents (more than one clause), the antecedents are evaluated using fuzzy operators (AND, OR and NOT) and consequently, a single number is produced. This number (the True value), as a result of antecedent, is then applied to the consequent membership function. The third step is the aggregation process where the membership functions of all rule consequences are combined into one fuzzy set and thereafter, an overall output is produced (Fig. 6c). Fuzzy model uses common inference methods such as the max-min method, the max-product method and the sum-product in aggregation and implication operations. The fuzzy aggregation operator is donated by either max or sum, while implication operator is exhibited by either min or prod [56]. The max-min inference method used in this study appropriately computed the fuzzy relations and provided good and expressive setting for constraint propagation. In this step, input variables including the list of membership functions are entered to aggregation process and the result is the generation of a single fuzzy set for every output variable. The aggregated outputs of the fuzzy set enter the defuzzification process (final step) and then, the defuzzifier converts them to a crisp number. Therefore, the obtained output of a fuzzy inference system is a single number. There are multiple defuzzification methods including the centroid, maximum, mean of maxima, height, and modified height defuzzifier. Among them, the centroid technique is considered as the most common method in which the center of gravity of the aggregated fuzzy set is calculated and returned. The mathematical equation of center of gravity (COG) is presented below:

$$COG = \frac{\int \mu_A(X) \cdot xd(x)}{\int \mu_A(X) \cdot dx} \tag{13}$$

where, $\mu_A(x)$ is the membership function of x in fuzzy set A.

Please cite this article as: H. Javadian et al., Using fuzzy inference system to predict Pb (II) removal from aqueous solutions by magnetic Fe_3O_4/H_2SO_4-activated *Myrtus Communis* leaves carbon nanocomposite, Journal of the Taiwan Institute of Chemical Engineers (2018), https://doi.org/10.1016/j.jtice.2018.06.021

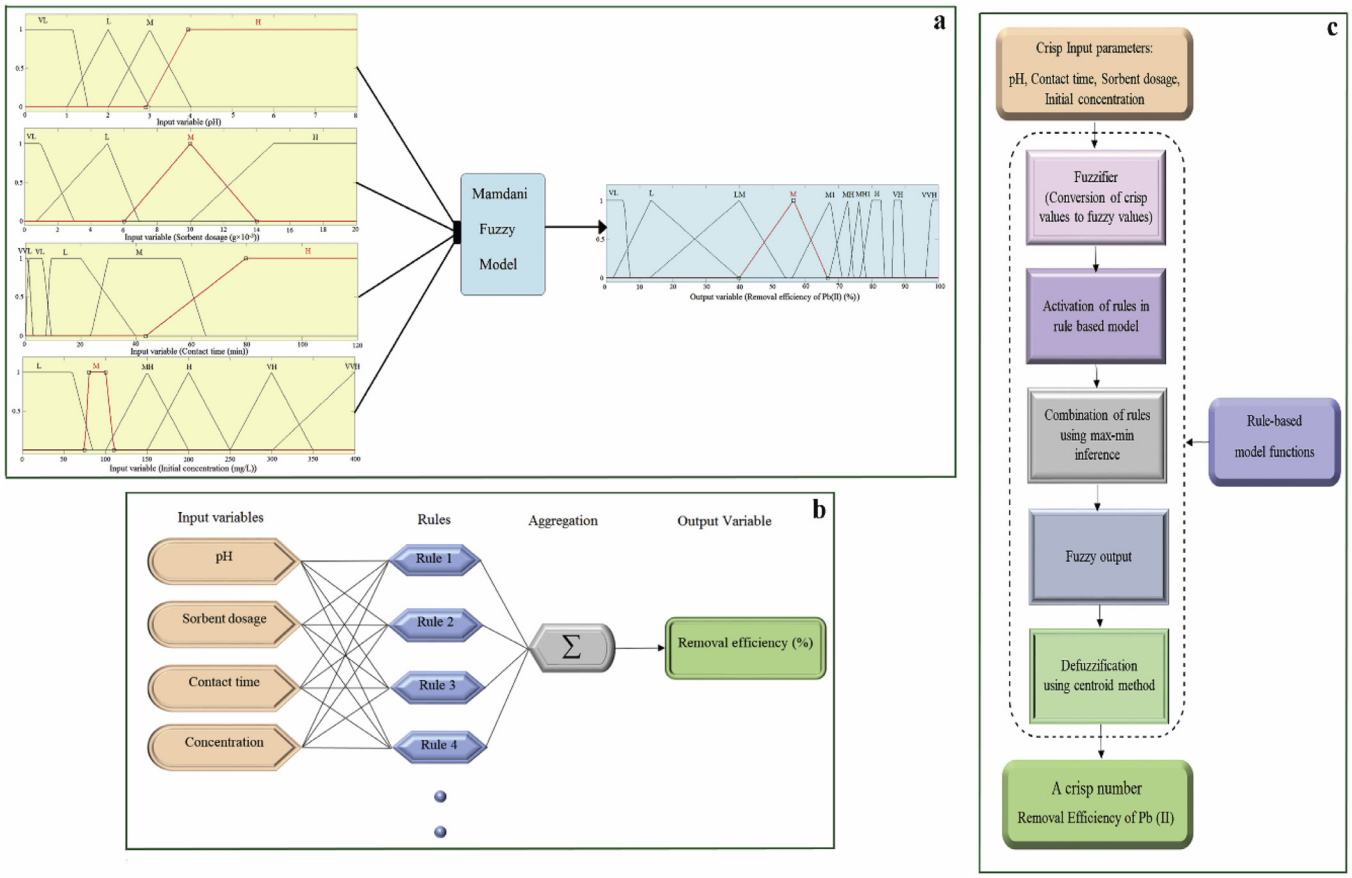

Fig. 6. (a) Membership functions of the input variables (pH, adsorbent dosage (g), contact time (min) and initial concentration of Pb(II) (mg/L)) and output (removal efficiency of Pb(II)), (b) input-output map for the prediction of Pb(II) removal efficiency in the proposed fuzzy inference system and (c) overview of fuzzy inference system.

3.9.2. Analysis of proposed model

Development of fuzzy logic model was efficiently carried out by transferring expert knowledge to the model in the form of 18 fuzzy IF-THEN rules and then, the developed model was applied to predict Pb (II) removal efficiency. As indicated in Fig. 7, the obtained fuzzy values of removal efficiency are plotted versus operating variables in a 3D diagram. The three dimensional surfaces of fuzzy rules show that increasing pH (Fig. 7a, b and f), contact time (Fig. 7a, c and d), and adsorbent dosage (Fig. 7b, c and e), increases Pb (II) removal efficiency. At optimum pH, by increasing contact time to 80 min, the values of removal efficiency are rapidly enhanced and thereafter, its growth rate decreases. This phenomenon clearly approves that the adsorption process is performed before 80 min particularly in the first 50 min. In the case of adsorbent dosage, it is obvious that by increasing this parameter, the removal efficiency increases due to the more accessibility of the vacant sites on the adsorbent surface. In contrast, by increasing the initial concentration of Pb (II) (Fig. 7d, e and f), the predicted values of removal efficiency decrease. The main reason for this reduction is that in lower concentrations, the porous surface of the adsorbent is saturated. As a result, the vacant sites on the adsorbent surface for Pb (II) adsorption considerably decrease. In summary, the maximum adsorption rate can be achieved under conditions of optimum pH, higher contact time and adsorbent dosage and lower initial concentration of Pb (II). As demonstrated in Fig. 7, the results of the developed model have a good agreement with the experimental data, affirming that the fuzzy logic model has an excellent performance in the prediction of the Pb (II) adsorption process.

3.9.3. Response of fuzzy logic model

In order to ascertain the response of fuzzy logic model, the predicted values of Pb (II) removal efficiency were plotted versus each input variables using Matlab software. As demonstrated in Fig. 8a, there is a small diversion between the predicted and experimental data in each plot which clearly confirms the high accuracy of the fuzzy model. Also, the model validation was conducted using liner regression as presented in Fig. 8b. According to this figure, it can be observed that the rule-based model provides a reasonably precise prediction except for a few data. The obtained coefficient of determination ($R^2 > 0.99$) proves that there is an excellent fitness between the predicted and experimental data. In addition, their comparison is indicated in Fig. 8c along with the full information of input variables for each point (removal efficiency). The performance of fuzzy model was verified using multiple important criteria comprising of mean squared normalized error (MSE), root mean squared error (RMSE), average relative error (ARE), absolute average relative error (AARE), standard deviation (SD), and coefficient of determination (R^2). Table 5 reports the values of MSE, RMSE, ARE, AARE, SD and R^2 obtained by the predicted fuzzy model. Results show that the proposed model has a high capability in predicting Pb (II) removal efficiency. The calculation of MSE, ARE, AARE, SD and R^2 was accomplished using the following equations:

$$MSE = \frac{1}{N}\sum_{i=1}^{n}\left(x_{Pb(II),pred} - x_{Pb(II),exp}\right)^2 \quad (14)$$

Please cite this article as: H. Javadian et al., Using fuzzy inference system to predict Pb (II) removal from aqueous solutions by magnetic Fe_3O_4/H_2SO_4-activated *Myrtus Communis* leaves carbon nanocomposite, Journal of the Taiwan Institute of Chemical Engineers (2018), https://doi.org/10.1016/j.jtice.2018.06.021

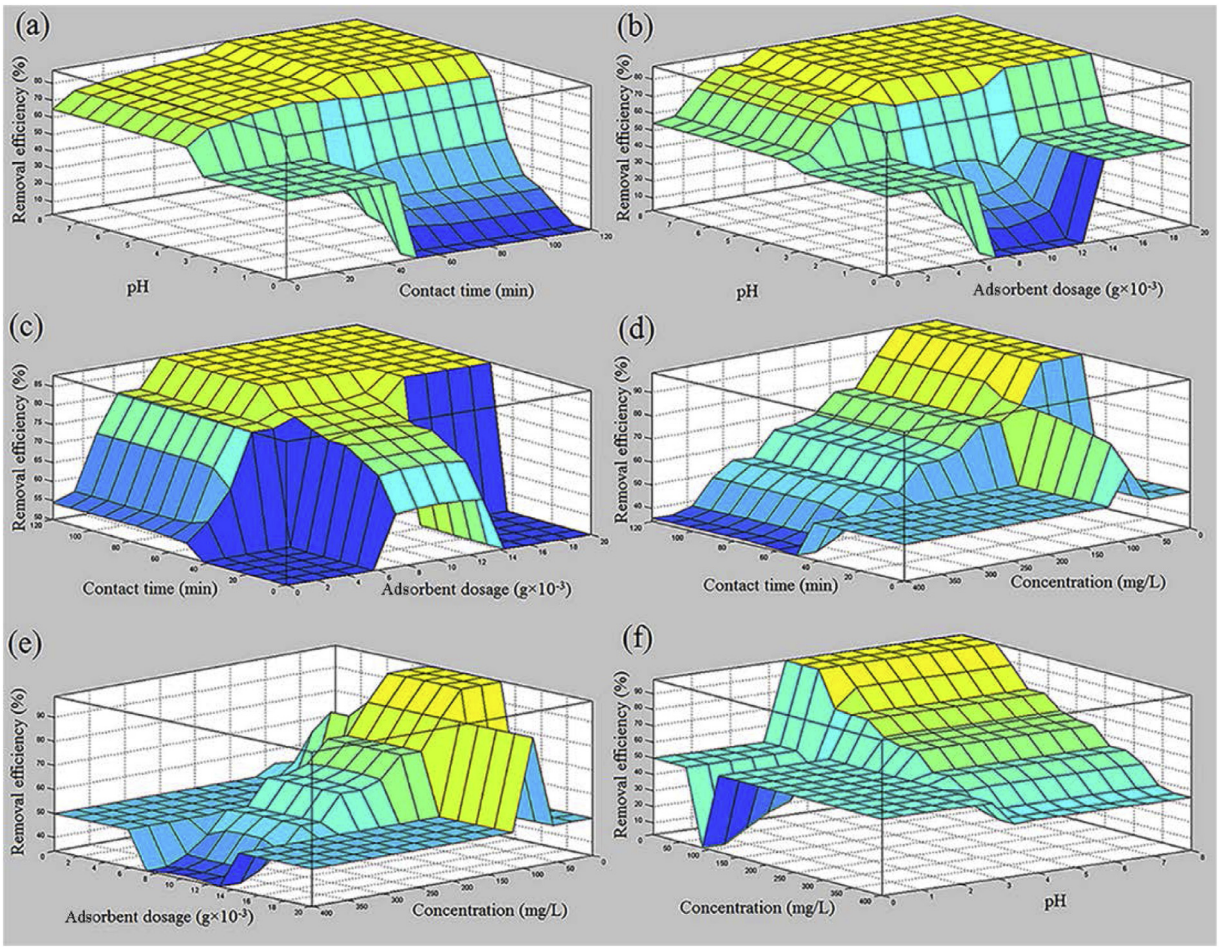

Fig. 7. Three dimensional surfaces of fuzzy model rules for the prediction of Pb (II) removal efficiency (a) pH and contact time, (b) pH and adsorbent dosage, (c) contact time and adsorbent dosage, (d) contact time and concentration, (e) adsorbent dosage and concentration and (f) concentration and pH.

Table 5
MSE, RMSE, ARE, AARE, SD and R^2 for Pb(II) removal efficiency obtained by the fuzzy logic model.

Response variable	Method	MSE	RMSE	% ARE	% AARE	% SD	R^2
Removal efficiency (%)	Fuzzy	3.7157	1.9276	0.59	2.24	2.92	0.9928

$$\mathrm{ARE} = \frac{1}{N}\sum_{i=1}^{N}\left(\frac{X_{exp(i)} - X_{pred(i)}}{X_{exp(i)}}\right) \quad (15)$$

$$\mathrm{AARE} = \frac{1}{N}\sum_{i=1}^{N}\left(\left|\frac{X_{exp(i)-X_{pred(i)}}}{X_{exp(i)}}\right|\right) \quad (16)$$

$$\mathrm{SD} = \sqrt{\frac{1}{N-1}\sum_{i=1}^{n}\left(\left|\frac{X_{exp(i)-X_{pred(i)}}}{X_{exp(i)}}\right| - AARE\right)^2}. \quad (17)$$

$$R^2 = \frac{\left(\sum_{i=1}^{n}\left(x_{Pb(II),\ exp} - \overline{x_{Pb(II),exp}}\right)\left(x_{Pb(II),pred} - \overline{x_{Pb(II),\ pred}}\right)\right)^2}{\sum_{i=1}^{n}\left(x_{Pb(II),exp} - \overline{x_{Pb(II),exp}}\right)^2\left(x_{Pb(II),pred} - \overline{x_{Pb(II),pred}}\right)^2} \quad (18)$$

Furthermore, the outcomes of several artificial intelligence techniques modeled for predicting the removal efficiency of various adsorbents were compared with the result of the proposed fuzzy logic model used in this study. The summery of information consisting of different adsorbents for the adsorption process, their modeling methods, and the coefficient of determination is shown in Table 6. In comparison with other models, the developed statistical model applied in this study shows an excellent performance with high accuracy in predicting Pb (II) removal efficiency. This reveals that the proposed fuzzy logic model has a remarkable ability in the identification of complex non-liner relationships between input-output variables in adsorption processes.

3.10. Sensitivity analysis

The sensitivity analysis was employed in order to diagnose the relative importance of each input variable on output variable in the predicted fuzzy model. The rate of changes of each input parameter in equal intervals of a given point was distinctly evaluated using sensitivity analysis under constant conditions of other input variables. It is obvious that each input parameter affects on the output parameter differently, because the rate of changes of removal efficiency at the determined point of each plot is different. As exhibited in Fig. 8d, the pH of aqueous solution has the highest impact on Pb (II) removal efficiency (approximately 51%). The results of sensitivity analysis show that contact time (~14%) and particularly adsorbent dosage (~8%) have lower effects on Pb (II) removal efficiency compared to pH and Pb (II) initial concentration. The main reason of this phenomenon could be inferred from the two-dimensional curves of each input variable versus removal efficiency. According to the plot of contact time versus

Please cite this article as: H. Javadian et al., Using fuzzy inference system to predict Pb (II) removal from aqueous solutions by magnetic Fe_3O_4/H_2SO_4-activated *Myrtus Communis* leaves carbon nanocomposite, Journal of the Taiwan Institute of Chemical Engineers (2018), https://doi.org/10.1016/j.jtice.2018.06.021

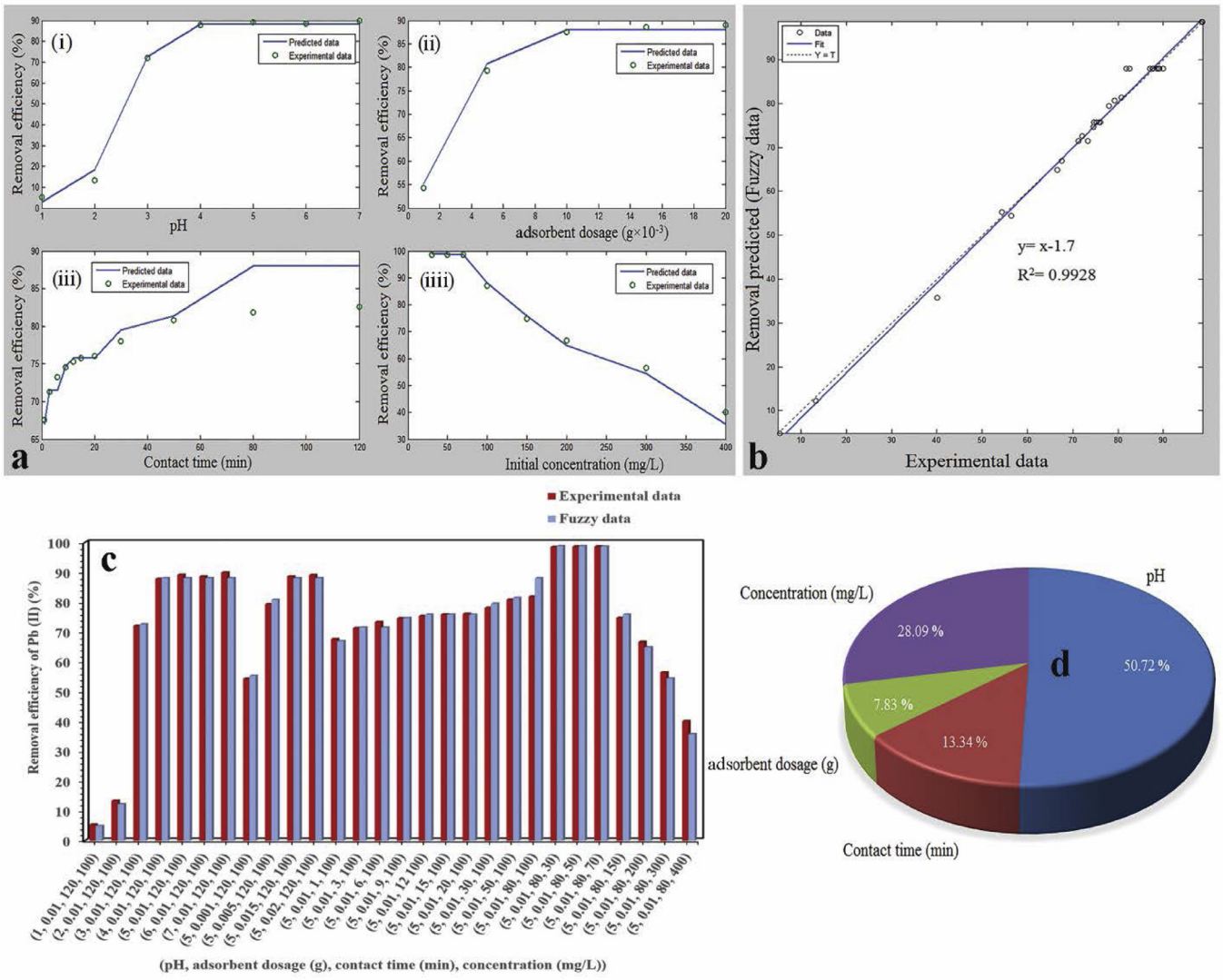

Fig. 8. (a) Response of fuzzy logic model (Pb(II) removal efficiency) related to (i) pH, (ii) adsorbent dosage ($g \times 10^{-3}$), (iii) contact time (min) and (iv) initial concentration (mg/L), (b) validation of the proposed fuzzy model using liner regression of fuzzy data related to the experimental data for Pb(II) removal efficiency, (c) comparison between the experimental and fuzzy data for Pb(II) removal efficiency and (d) sensitivity of Pb(II) removal efficiency toward each input variable.

Table 6
Performance comparison of the prediction models reported in the literatures and the proposed fuzzy logic model for Pb(II) removal.

Adsorbent	Method	Response variable	Statistical index	Ref.
Active carbon (AC)	ANN	Pure and binary gas absorption	$R^2 = 0.997$	[57]
ZnS nanoparticle	ANN-PSO	BG dye removal	$R^2_{ANN\text{-}PSO} = 0.9610$	[58]
loaded on AC	MLR		$R^2_{MLR} = 0.9231$	
AC	ANN	SY dye removal	$R^2 = 0.998$	[59]
Cu nanowires	ANN, MLR	Malachite green	$R^2_{ANN} = 0.9658$	[60]
loaded on AC		(MG) removal	$R^2_{MLR} = 0.8133$	
AC	$RSM_{(CCD)}$	4-CP removal	$R^2 = 0.949$	[61]
Fe_2O_3–ZnO–$ZnFe_2O_4$/carbon nano-composite	$RSM_{(CCD)}$	BPB dye removal	$R^2_{CCD} = 0.9947$	[62]
SnS-NP-AC	RF	CR dye removal	$R^2 = 0.9793$	[25]
CuO–ZnO nano-composite (FCZN)	GP	DR23, DR80 and DR81 dyes removal	$R^2_{DR23} = 0.9837$	[63]
			$R^2_{DR80} = 0.9616$	
			$R^2_{DR81} = 0.9763$	
MM-AC	Fuzzy	Pb(II) removal	$R^2 = 0.9928$	This study

removal efficiency, it can be observed that the adsorption process is considerably performed at the beginning of the process *i.e.* the first 50 min (steep slope) and then, the rate of adsorption decreases (mild slope). Also, the low importance of adsorbent dosage compared to the other input variables can be interpreted using the plot of adsorbent dosage versus removal efficiency. It shows that most of Pb (II) ions are adsorbed at low dosage of the MM-AC (less than 0.005 g); thereafter, the rate of removal efficiency declines.

3.11. Possible applicability of the MM-AC in a full-scale operation

There are two important factors including cheapness and effectiveness for the application of an adsorbent in a full-scale op-

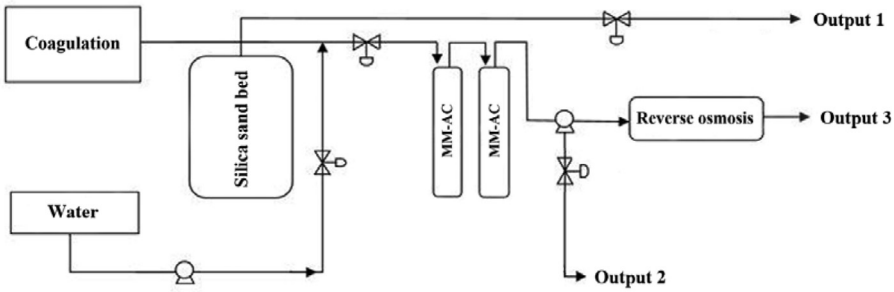

Scheme 2. Process flow diagram (PFD) of a common large-scale wastewater treatment unit.

eration. As long as *Myrtus Communis* abundance and its properties have attracted the attention of the related industries, it is expected that a large amounts of waste material from *Myrtus Communis* to be generated in the close future as a by-product after the processes like extraction process. The outcomes of this study clearly demonstrated that the *Myrtus Communis* derived active carbon (M-AC) can be converted to an efficient adsorbent (MM-AC). Basically, an efficient wastewater treatment unit in both pilot and industrial scales is consisting of a series of successive separation operations such as electrocoagulation, flotation, adsorption, reverse osmosis, etc. The adsorption step is one of the main parts of sequestration process that is usually performed in two sub-parts including silica sand bed and active carbon filters. The high uptake capacity of an adsorbent in the real operational conditions plays a significant role in the whole process. This investigation showed that the MM-AC efficiently removed Pb (II) from aqueous solutions by considering a very low dosage (0.005 g) and appropriate adsorption time (80 min) at high Pb (II) initial concentration. These results are indicative that it can be utilized as an efficient and cost-effective adsorbent in a full-scale operation. In addition, the adsorption behavior of the MM-AC was predicted by an artificial intelligence-based approach. The low deviation of the predicted data from the experimental data confirmed that the adsorption process of Pb (II) by the MM-AC is applicable in a large-scale operation. The adsorption capacity of the MM-AC was determined by the reusability studies to confirm its ability as a powerful adsorbent. The evaluations illustrated that the proposed adsorbent can effectively remove Pb (II) from aqueous solution (up to 70%) after consecutive adsorption-desorption cycles. The MM-AC can be used in an actual wastewater treatment unit like Scheme 2 to give satisfactory results such as obtaining higher removal efficiency, decreasing dependence on reverse osmosis (RO) step, increasing the lifetime of AC and RO filters, decreasing the operational costs, and ultimately the production of cleared wastewater within a lower time.

4. Conclusions

In this research, a magnetic nanocomposite consisting of the Fe_3O_4 nanoparticles immobilized on *Myrtus Communis*-derived activated carbon (MM-AC) was synthesized and characterized by FE-SEM and FT-IR analytical methods. The created activated carbon was porous with the holes in different sizes. The sizes of the Fe_3O_4 particles immobilized on the activated carbon were about 54 nm. The changes in the peak intensities showed that the binding process was occurred on the surface of the adsorbent. Different factors such as solution pH, adsorbent dosage, contact time and Pb (II) initial concentration were investigated, and more than 89% of Pb (II) was removed at optimum conditions. The adsorption kinetic studies illustrated that the experimental data can be well described by pseudo-second-order model. The equilibrium data can be well fitted to Langmuir type 1 model, and the maximum monolayer adsorption capacity of the MM-AC was obtained to be 500 mg/g. After five cycles of adsorption–desorption using 0.1 M HCl, the removal efficiency decreased from 87.30 to 81.55%. In addition, Pb (II) removal efficiency by the adsorbent was predicted based on operational parameters examined in actual conditions of the experiments. A Mamdani type of fuzzy inference system was developed using 18 IF-THEN rules along with eight levels of both trapezoidal and triangular membership functions. The fuzzy logic model showed a highly accurate prediction with $R^2 > 0.99$. For future studies, in order to achieve more precise results of both predicted and experimental data, the effects of other important input variables such as rotation speed and volume of solution should be investigated. In addition, the combination of other types of membership functions (MFs) can be applied in fuzzy logic subsets to obtain an accurate prediction of Pb (II) removal efficiency. In summary, according to the assessments carried out on both experimental and predicted data, the prepared magnetic nanocomposite can be considered as an effective adsorbent for Pb (II) removal from aqueous solutions.

Acknowledgments

This work has been supported by the Spanish Ministry of Economy and Competitiveness (Ref. CTM2017-83581-R). Hamedreza Javadian acknowledges the financial support received (Ref. BES-2015-072506).

References

[1] Javadian H, Vahedian P, Toosi M. Adsorption characteristics of Ni(II) from aqueous solution and industrial wastewater onto polyaniline/HMS nanocomposite powder. Appl Surf Sci 2013;284:13–22.
[2] Javadian H, Zamani Sorkhrodi F, Babzadeh Koutenaei B. Experimental investigation on enhancing aqueous cadmium removal via nanostructure composite of modified hexagonal type mesoporous silica with polyaniline/polypyrrole nanoparticles. J Ind Eng Chem 2014;20:3678–88.
[3] Ghasemi M, Naushad Mu, Ghasemi N, Khosravi-fard Y. A novel agricultural waste based adsorbent for the removal of Pb(II) from aqueous solution: kinetics, equilibrium and thermodynamic studies. J Ind Eng Chem 2014;20:454–61.
[4] Javadian H, Babzadeh Koutenaei B, Shekarian E, Zamani Sorkhrodi F, Khatti R, Toosi M. Application of functionalized nano HMS type mesoporous silica with N-(2-aminoethyl)-3-aminopropyl methyldimethoxysilane as a suitable adsorbent for removal of Pb (II) from aqueous media and industrial wastewater. J Saudi Chemical Soc 2017;21:S219–30.
[5] Javadian H, Ghasemi M, Ruiz M, Sastre AM, Hosseini Asl SM, Masomi M. Fuzzy logic modeling of Pb (II) sorption onto mesoporous NiO/$ZnCl_2$-*Rosa Canina-L* seeds activated carbon nanocomposite prepared by ultrasound-assisted co-precipitation technique. Ultrason Sonochem 2018;40(A):748–62.
[6] Ghasemi M, Zeinaly Khosroshahy M, Bavand Abbasabadi A, Ghasemi N, Javadian H, Fattahi M. Microwave-assisted functionalization of *Rosa Canina-L* fruits activated carbon with tetraethylenepentamine and its adsorption behavior toward Ni(II) in aqueous solution: kinetic, equilibrium and thermodynamic studies. Powder Technol 2015;274:362–71.
[7] Moussavi G, Barikbin B. Biosorption of chromium (VI) from industrial wastewater onto pistachio hull waste biomass. Chem Eng J 2010;162:893–900.
[8] Singh KP, Gupta S, Singh AK, Sinha S. Optimizing adsorption of crystal violet dye from water by magnetic nanocomposite using response surface modeling approach. J Hazard Mater 2011;186:1462–73.
[9] Wang T, Jin X, Chen Z, Megharaj M, Naidu R. Simultaneous removal of Pb(II) and Cr(III) by magnetite nanoparticles using various synthesis conditions. J Ind Eng Chem 2014;20:3543–9.

Please cite this article as: H. Javadian et al., Using fuzzy inference system to predict Pb (II) removal from aqueous solutions by magnetic Fe_3O_4/H_2SO_4-activated *Myrtus Communis* leaves carbon nanocomposite, Journal of the Taiwan Institute of Chemical Engineers (2018), https://doi.org/10.1016/j.jtice.2018.06.021

[10] Nassar NN. Rapid removal and recovery of Pb(II) from wastewater by magnetic nanoadsorbents. J Hazard Mater 2010;184:538–46.
[11] Singh S, Barick1 KC, Bahadur D. Surface engineered magnetic nanoparticles for removal of toxic metal ions and bacterial pathogens. J Hazard Mater 2011;192:1539–47.
[12] Ge F, Li MM, Ye H, Zhao BX. Effective removal of heavy metal ions Cd^{2+}, Zn^{2+}, Pb^{2+}, Cu^{2+} from aqueous solution by polymer-modified magnetic nanoparticles. J Hazard Mater 2012;211–212:366–72.
[13] Xu P, Zeng GM, Huang DL, Lai C, Zhao MH, Wei Z, Li NJ, Huang C, Xie GX. Adsorption of Pb(II) by iron oxide nanoparticles immobilized *Phanerochaete chrysosporium*: equilibrium, kinetic, thermodynamic and mechanisms analysis. Chem Eng J 2012;203:423–31.
[14] Lee SM, Laldawngliana C, Tiwari D. Iron oxide nano-particles-immobilized-sand material in the treatment of Cu(II), Cd(II) and Pb(II) contaminated waste waters,. Chem Eng J 2012;195–196:103–11.
[15] Jabeen H, Kemp KC, Chandra V. Synthesis of nano zerovalent iron nanoparticles e Graphene composite for the treatment of lead contaminated water. J Environ Manage 2013;130:429–35.
[16] Xu P, Zeng G, Huang D, Hu S, Feng C, Lai C, Zhao M, Huang C, Li N, Wei Z, Xie G. Synthesis of iron oxide nanoparticles and their application in *Phanerochaete chrysosporium* immobilization for Pb(II) removal. Colloids Surf A Physicochem Eng Aspects 2013;419:147–55.
[17] Tran HV, Tran LD, Nguyen TN. Preparation of chitosan/magnetite composite beads and their application for removal of Pb(II) and Ni(II) from aqueous solution,. Mater Sci Eng C 2010;30:304–10.
[18] Pereira P, Bernardo-Gil MG, João Cebola M, Mauricio E, Romano A. Supercritical fluid extracts with antioxidant and antimicrobial activities from myrtle (*Myrtus Communis L.*) leaves. Response surface optimization. J Supercrit Fluids 2013;83:57–64.
[19] Rahimmalek M, Mirzakhani M, Ghasemi Pirbalouti A. Essential oil variation among 21 wild myrtle (*Myrtus communis L.*) populations collected from different geographical regions in Iran. Ind Crops Prod 2013;51:328–33.
[20] Ghaedi M, Tavallali H, Sharifi M, Nasiri Kokhdan S, Asghari A. Preparation of low cost activated carbon from *Myrtus communis* and pomegranate and their efficient application for removal of congo red from aqueous solution. Spectrochim Acta Part A 2012;86:107–14.
[21] Badrnezhad R, Mirza B. Modeling and optimization of cross-flow ultrafiltration using hybrid neural network-genetic algorithm approach. J Ind Eng Chem 2014;20:528–43.
[22] Hosseini Asl SM, Ahmadi M, Ghiasvand M, Tardast A, Katal R. Artificial neural network (ANN) approach formodeling of Cr(VI) adsorption from aqueous solution byzeolite prepared from raw fly ash (ZFA). J Ind Eng Chem 2013;19:1044–55.
[23] Mandal S, Mahapatra SS, Patel RK. Neuro fuzzy approach for arsenic(III) and chromium(VI) removal from water. J Water Process Eng 2015;5:58–75.
[24] Ghaedi M, Ghaedi AM, Hossainpour M, Ansari A, Habibi MH, Asghari AR. Least square support vector (LS-SVM) method for modeling of methylene blue dye adsorption using copper oxide loaded on activated carbon: kinetic and isotherm study. J Ind Eng Chem 2014;25:1641–9.
[25] Dehghanian N, Ghaedi M, Ansari A, Ghaedi A, Vafaei A, Asif M, Agarwal S, Tyagi I, Gupta VK. A random forest approach for predicting the removal of congo red from aqueous solutions by adsorption onto tin sulfide nanoparticles loaded on activated carbon. Desalin Water Treat 2016;57:9272–85.
[26] Hajati S, Ghaedi M, Mazaheri H. Removal of methylene blue from aqueous solution by walnut carbon: optimization using response surface methodology. Desalin Water Treat 2014;52:1–15.
[27] Ghaedi M, Zeinali N, Ghaedi AM, Teimuori M, Tashkhourian J. Artificial neural network genetic algorithm based optimization for the adsorption of methylene blue and brilliant green from aqueous solution by graphite oxide nanoparticle. Spectrochim Acta A Mol Biomol Spectrosc 2014;125:264–77.
[28] Rahmanian B, Pakizeh M, Esfandyari M, Maskooki A. Fuzzy inference system for modeling of zinc removal using micellar-enhanced ultrafiltration. Sep Sci Technol 2011;46:1571–81.
[29] Zadeh LA. Fuzzy sets. Inf Control 1965;8:338–53.
[30] Gharibi H, Mahvi AH, Nabizadeh R, Arabalibeik H, Yunesian M, Sowlat MH. A novel approach in water quality assessment based on fuzzy logic. J Environ Manage 2012;112:87–95.
[31] Hosseini Asl SM, Masomi M, Hosseini M, Javadian H, Ruiz M, Sastre AM. Synthesis of hydrous iron oxide/aluminum hydroxide composite loaded on coal fly ash as an effective mesoporous and low-cost sorbent for Cr (VI) sorption: fuzzy logic modeling. Process Saf Environ Prot 2017;107:153–67.
[32] Rahmanian B, Pakizeh M, Esfandyari M, Heshmatnezhad F, Maskooki A. Fuzzy modeling and simulation for lead removal using micellar-enhanced ultrafiltration (MEUF). J Hazard Mater 2011;192:585–92.
[33] Javadian H, Ghorbani F, Tayebi H, Hosseini Asl S. Study of the adsorption of Cd (II) from aqueous solution using zeolite-based geopolymer, synthesized from coal fly ash: kinetic, isotherm and thermodynamic studies. Arab J Chem 2015;8(6):837–49.
[34] Javadian H, Torabi Angaji M, Naushad M. Synthesis and characterization of polyaniline/γ-alumina nanocomposite: a comparative study for the adsorption of three different anionic dyes. J Ind Eng Chem 2014;20(5):3890–900.
[35] Taheri R, Bahramifar N, Zarghami MR, Javadian H, Mehraban Z. Nanospace engineering and functionalization of MCM-48 mesoporous silica with dendrimer amines based on [1,3,5]-triazines for selective and pH-independent sorption of silver ions from aqueous solution and electroplating industry wastewater. Powder Technol 2017;321:44–54.
[36] Javadian H. Application of kinetic, isotherm and thermodynamic models for the adsorption of Co(II) ions on polyaniline/polypyrrole copolymer nanofibers from aqueous solution. J Ind Eng Chem 2014;20:4233–41.
[37] Ghasemi M, Ghasemi N, Zahedi G, Alwi SRW, Goodarzi M, Javadian H. Kinetic and equilibrium study of Ni(II) sorption from aqueous solutions onto Peganum harmala-L. Int J Environ Sci Technol 2014;11:1835–44.
[38] Ghasemi M, Javadian H, Ghasemi N, Agarwal S, Gupta VK. Microporous nanocrystalline NaA zeolite prepared by microwave assisted hydrothermal method and determination of kinetic, isotherm and thermodynamic parameters of the batch sorption of Ni (II). J Mol Liq 2016;215:161–9.
[39] Ross TJ. Fuzzy logic with engineering applications. John Wiley & Sons; 2009.
[40] Mamdani EH, Assilian S. An experiment in linguistic synthesis with a fuzzy logic controller. Int J Man Mach Stud 1975;7:1–13.
[41] Takagi T, Sugeno M. Fuzzy identification of systems and its application to modeling and control. IEEE Trans Syst Man Cybern 1985;15:116–32.
[42] Klir G, Yuan B. Fuzzy sets and fuzzy logic, 4. NJ: Prentice hall; 1995.
[43] Sathishkumar P, Arulkumar M, Palvannan T. Utilization of agro-industrial waste Jatropha curcas pods as an activated carbon for the adsorption of reactive dye Remazol Brilliant Blue R (RBBR). J Clean Prod 2012;22:67–75.
[44] Rohani Bastami T, Entezari MH. Activated carbon from carrot dross combined with magnetite nanoparticles for the efficient removal of p-nitrophenol from aqueous solution. Chem Eng J 2012;210:510–19.
[45] Panneerselvam P, Morad N, Tan KA. Magnetic nanoparticle (Fe_3O_4) impregnated onto tea waste for the removal of nickel (II) from aqueous solution. J Hazard Mater 2011;186:160–8.
[46] Hajeeth T, Vijayalakshmi K, Gomathi T, Sudha PN. Removal of Cu(II) and Ni(II) using cellulose extracted from sisal fiber and cellulose-g-acrylic acid copolymer. Int J Biol Macromol 2013;62:59–65.
[47] Shin KY, Hong JY, Jang J. Heavy metal ion adsorption behavior in nitrogen–doped magnetic carbon nanoparticles: isotherms and kinetic study. J Hazard Mater 2011;190:36–44.
[48] Zhang S, Yang H, Huang H, Gao H, Wang X, Cao R, Li J, Xu X, Wang X. Unexpected ultrafast and high adsorption capacity of oxygen vacancy-rich WOx/C nanowire networks for aqueous Pb^{2+} and methylene blue removal. J Mater Chem A 2017;5:15913–22.
[49] Du Y, Wang J, Zou Y, Yao W, Hou J, Xia L, Peng A, Alsaedi A, Hayat T, Wang X. Synthesis of molybdenum disulfide/reduced graphene oxide composites for effective removal of Pb(II) from aqueous solutions. Science Bulletin 2017;62:913–22.
[50] Huang S, Song S, Zhang R, Wen T, Wang X, Yu S, Song W, Hayat T, Alsaedi A, Wang X. Construction of layered double hydroxides/hollow carbon microsphere composites and its applications for mutual removal of Pb(II) and humic acid from aqueous solutions,. ACS Sustain Chem. Eng 2017;5:11268–79.
[51] Tang C, Shu Y, Zhang R, Li X, Song J, Li B, Zhang Y, Oua D. Comparison of the removal and adsorption mechanisms of cadmium and lead from aqueous solution by activated carbons prepared from *Typha angustifolia* and *Salix matsudana*. RSC Adv 2017;7:16092–103.
[52] Idris A, Suriani Mohd Ismail N, Hassan N, Misran E, Ngomsik AF. Synthesis of magnetic alginate beads based on maghemite nanoparticles for Pb (II) removal in aqueous solution. J Ind Eng Chem 2012;18:1582–9.
[53] Tan Y, Chen M, Hao Y. High efficient removal of Pb (II) by amino-functionalized Fe_3O_4 magnetic nano-particles. Chem Eng J 2012;191:104–11.
[54] Zhang J, Zhai S, Li S, Xiao Z, Song Y, An Q, Tian G. Pb(II) removal of Fe_3O_4@SiO_2–NH_2 core–shell nanomaterials prepared via a controllable sol–gel process, Chem. Eng J 2013;215–216:461–71.
[55] Kosco B. Fuzzy thinking: the new science of fuzzy logic. NY: Hyperion; 1993.
[56] Sivanandam SN. Introduction to fuzzy logic using MATLAB. Berlin: Springer; 2007.
[57] Fotoohi F, Iranagh SA, Golzar K, Modarress H. Predicting pure and binary gas adsorption on activated carbon with two-dimensional cubic equations of state (2-D EOSs) and artificial neural network (ANN) method. Phys Chem Liq 2016;54:281–302.
[58] Ghaedi M, Ansari A, Bahari F, Ghaedi AM, Vafaei A. A hybrid artificial neural network and particle swarm optimization for prediction of removal of hazardous dye brilliant green from aqueous solution using zinc sulfide nanoparticle loaded on activated carbon. Spectrochim Acta Part A 2015;137:1004–15.
[59] Ghaedi AM, Ghaedi M, Karami P. Comparison of ultrasonic with stirrer performance for removal of sunset yellow (SY) by activated carbon prepared from wood of orange tree: artificial neural network modeling. Spectrochim Acta Part A 2015;138:789–99.
[60] Ghaedi M, Shojaeipour E, Ghaedi AM, Sahraei R. Isotherm and kinetics study of malachite green adsorption onto copper nanowires loaded on activated carbon: artificial neural network modeling and genetic algorithm optimization. Spectrochim Acta Part A 2015;142:135–49.
[61] Noorimotlagh Z, Shahriyar S, Soltani RDC, Tajik R. Optimized adsorption of 4-chlorophenol onto activated carbon derived from milk vetch utilizing response surface methodology. Desalin Water Treat 2016;30:14213–26.
[62] Mohammadzadeh A, Ramezani M, Ghaedi AM. Synthesis and characterization of Fe_2O_3-ZnO-$ZnFe_2O_4$/carbon nanocomposite and its application to removal of bromophenol blue dye using ultrasonic assisted method: optimization by response surface methodology and genetic algorithm. J Taiwan Inst Chem Eng 2016;59:275–84.
[63] Mahmoodi NM, Chamani H, Kariminia HR. Functionalized copper oxide–zinc oxide nanocomposite: synthesis and genetic programming model of dye adsorption. Desalin Water Treat 2016;40:18755–69.

Please cite this article as: H. Javadian et al., Using fuzzy inference system to predict Pb (II) removal from aqueous solutions by magnetic Fe_3O_4/H_2SO_4-activated *Myrtus Communis* leaves carbon nanocomposite, Journal of the Taiwan Institute of Chemical Engineers (2018), https://doi.org/10.1016/j.jtice.2018.06.021